Expanded View Figures

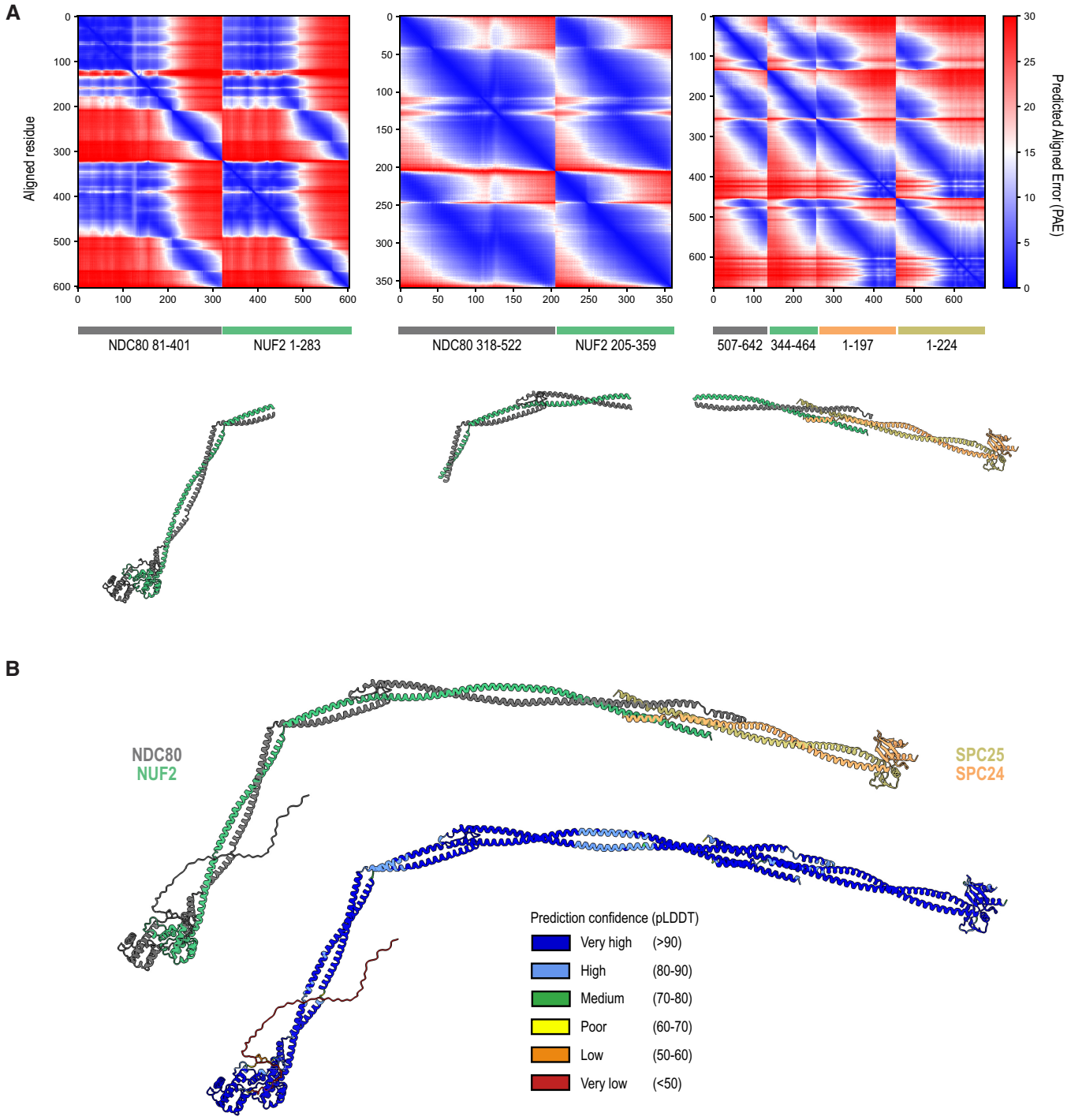

Figure EV1.

◀ **Figure EV1. Structural *in silico* analysis of the human Ndc80 complex.**

A Boundaries and Predicted Aligned Error (PAE) scores of the three Ndc80 segments that were predicted by AF2 multimer. These fragments were used to generate a composite prediction of the full-length Ndc80 complex. More information can be found in the Materials and Methods section.

B The prediction of the full-length Ndc80 complexes with colors representing the different subunits (as in Fig 1B) and the local prediction confidence intervals.

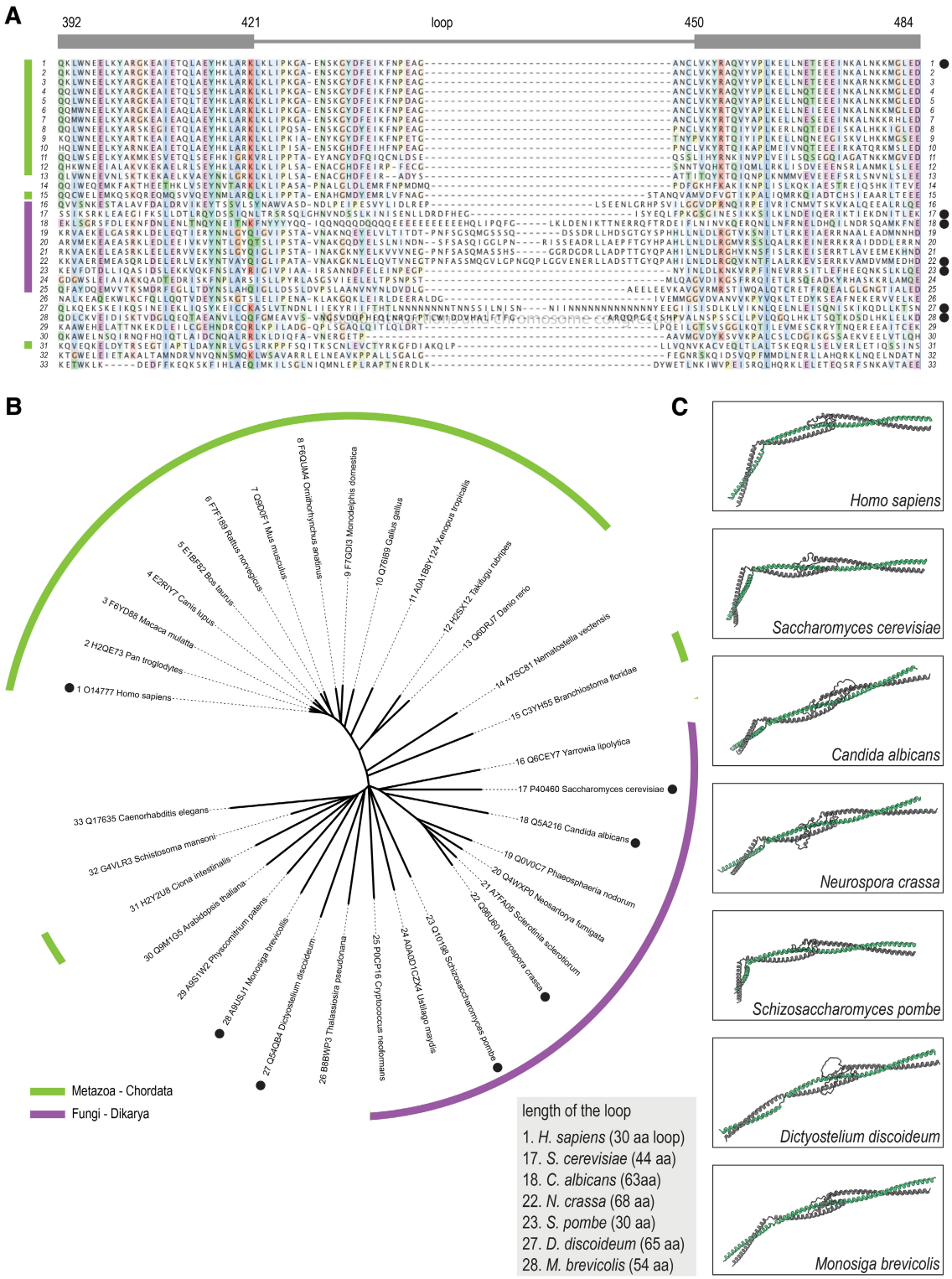
A
392
421
loop
450
484
B
1 O14777 Homo sapiens
2 H2QE73 Pan troglodytes
3 F6YD88 Macaca mulatta
4 E2RIY7 Canis lupus
5 E1BF92 Bos taurus
6 F7F189 Rattus norvegicus
7 Q9DBF1 Mus musculus
8 F6QUM4 Ornithorhynchus anatinus
9 F7GDI3 Monodelphis domestica
10 Q7T6B9 Gallus gallus
11 A0A1B8Y124 Xenopus tropicalis
12 H2SX12 Takifugu rubripes
13 Q6DRJ7 Danio rerio
14 A7SC81 Nematostella vectensis
15 C3YH55 Branchiostoma floridae
16 Q6CEY7 Yarrowia lipolytica
17 P40460 Saccharomyces cerevisiae
18 Q5A216 Candida albicans
19 Q0V0C7 Phaeosphaeria nodorum
20 Q4WXP0 Neosartorya fumigata
21 A7F5A05 Sclerotinia sclerotiorum
22 Q8X060 Neurospora crassa
23 Q10198 Schizosaccharomyces pombe
24 A0A0D1CZX4 Ustilago maydis
25 PNCP16 Cryptococcus neoformans
26 B8BWP3 Thalassiosira pseudonana
27 Q5K0B4 Dictyostelium discoideum
28 A9USJ1 Monosiga brevicollis
29 A9S1W2 Physcomitrium patens
30 Q9M1G5 Arabidopsis thaliana
31 H2YZU8 Ciona intestinalis
32 G4VLR3 Schistosoma mansoni
33 Q17635 Caenorhabditis elegans
Metazoa - Chordata
Fungi - Dikarya
length of the loop
1. H. sapiens (30 aa loop)
17. S. cerevisiae (44 aa)
18. C. albicans (63aa)
22. N. crassa (68 aa)
23. S. pombe (30 aa)
27. D. discoideum (65 aa)
28. M. brevicolis (54 aa)
C
Homo sapiens
Saccharomyces cerevisiae
Candida albicans
Neurospora crassa
Schizosaccharomyces pombe
Dictyostelium discoideum
Monosiga brevicolis

Figure EV2.

Figure EV2. Alignments, phylogenetic tree, and structural conservation of the Ndc80 kink and loop.

A Sequence alignment of the loop region of the NDC80 subunit in various species. Residue numbers correspond to the human NDC80.

B Unrooted phylogenetic tree that was generated with complete NDC80 sequences. Sequences in panel (A) were arranged according to this tree. Species belonging to the Chordata phylum (light green) and the Fungi kingdom (purple) are indicated. Black dots mark species for which we predicted the structure.

C Predicted structures of the NDC80:NUF2 region spanning the hinge and loop regions. Shown in similar orientations following structural alignment to the human fragment $NDC80^{376–516}$:$NUF2^{269–356}$.

Source data are available online for this figure.

Figure EV3. Electroporation efficiency and a comparison of loop mutants.

A Immunofluorescence quantification of Ndc80, KNL1, and NSL1 at kinetochores following electroporation of different Ndc80 constructs. The number of kinetochores analyzed for NDC80: wt - 758, ΔL - 2,053, M5 - 1,612, KNL1: wt - 697, ΔL - 635, M5 - 602, and NSL1: wt - 647, ΔL - 644, M5 - 611. Red lines indicate median value with interquartile range.

B Schematic representation of the predicted structure of the NDC80:NUF2 loop region with annotations to illustrate residues with side-chains that pack a hydrophobic core and mutants that interfere with chromosome congression as illustrated in Fig 4E and Wimbish *et al* (2020).

C Immunofluorescence quantification of various kinetochore proteins in cells that were treated as described in panel (A), but with nocodazole added 15 h after electroporation and 3 h before fixation. The number of kinetochores analyzed for CENP-T: wt - 799, ΔL - 750, M5 - 855, BUB1: wt - 2,226, ΔL - 1,993, M5 - 1,598, and BUBR1: wt - 2,315, ΔL - 2,112, M5 - 1,549. Red lines indicate median value with interquartile range.

D A new anti-SKA antibody, generated against the full-length recombinant SKA complex, mainly recognizes SKA3 in a HeLa cell lysate using immunoblotting. Asterisks indicate non-specific bands that are not sensitive to depletion of the SKA complex by RNAi.

E–G The antibody also recognizes SKA by immunofluorescence. SKA levels are higher in MG132 arrested cells than in STLC or nocodazole arrested cells. Scale bar: 5 μm.

H, I SKA levels recruited to kinetochores in nocodazole-exposed cells with various Ndc80 complexes. Scale bar: 5 μm.

Source data are available online for this figure.

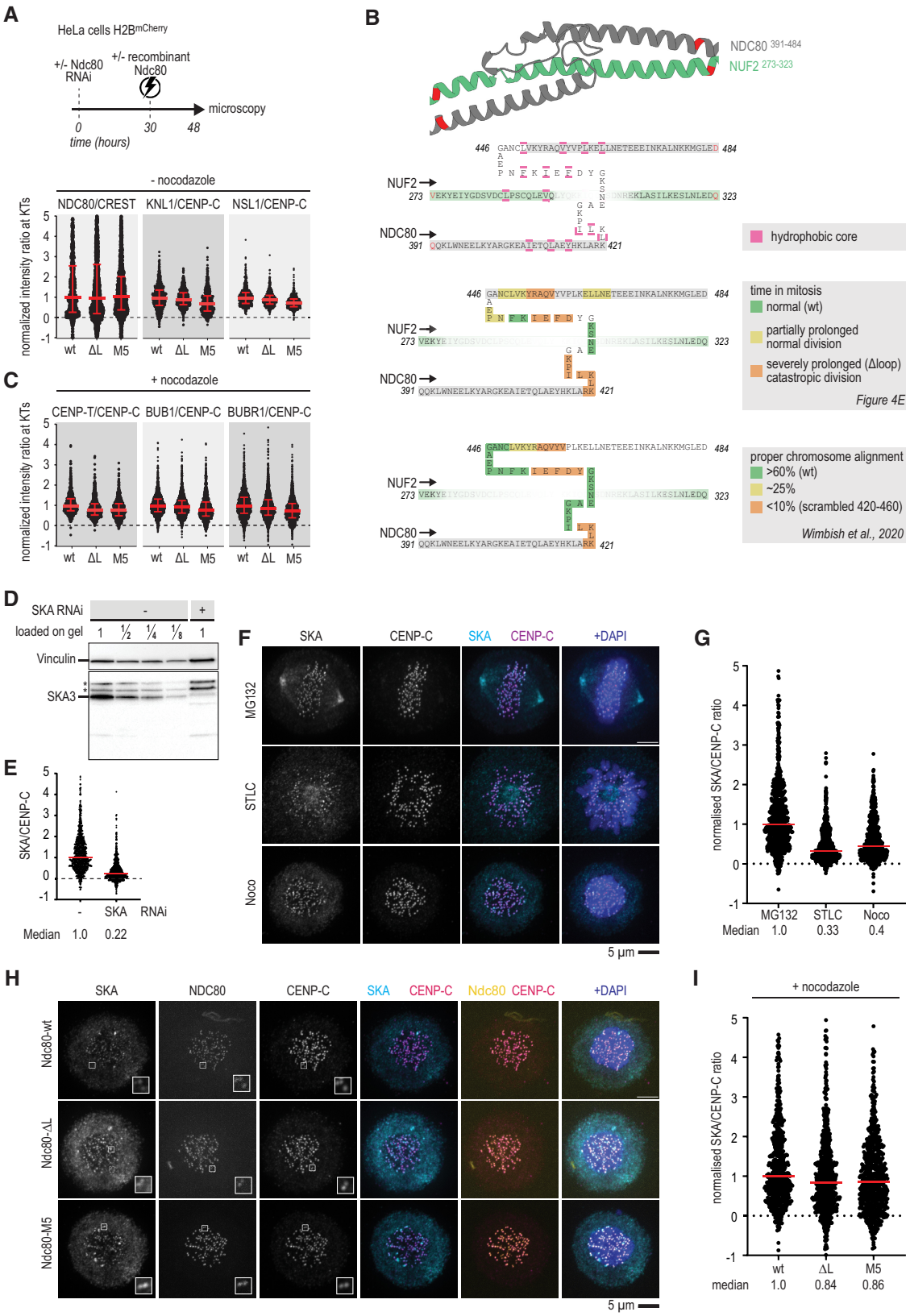
A
HeLa cells H2B^mCherry
+/- Ndc80 RNAi
+/- recombinant Ndc80
microscopy
0
30
48
time (hours)
- nocodazole
NDC80/CREST
KNL1/CENP-C
NSL1/CENP-C
normalized intensity ratio at KTs
wt ΔL M5
C
+ nocodazole
CENP-T/CENP-C
BUB1/CENP-C
BUBR1/CENP-C
B
NDC80 391-484
NUF2 273-323
hydrophobic core
time in mitosis
normal (wt)
partially prolonged normal division
severely prolonged (Δloop) catastropic division
Figure 4E
proper chromosome alignment
>60% (wt)
~25%
<10% (scrambled 420-460)
Wimbish et al., 2020
D
SKA RNAi
loaded on gel
Vinculin
SKA3
E
SKA/CENP-C
Median 1.0 0.22
F
SKA
CENP-C
+DAPI
MG132
STLC
Noco
5 μm
G
normalised SKA/CENP-C ratio
MG132 STLC Noco
Median 1.0 0.33 0.4
H
NDC80
Ndc80 CENP-C
Ndc80-wt
Ndc80-ΔL
Ndc80-M5
I
median 1.0 0.84 0.86

Figure EV3.

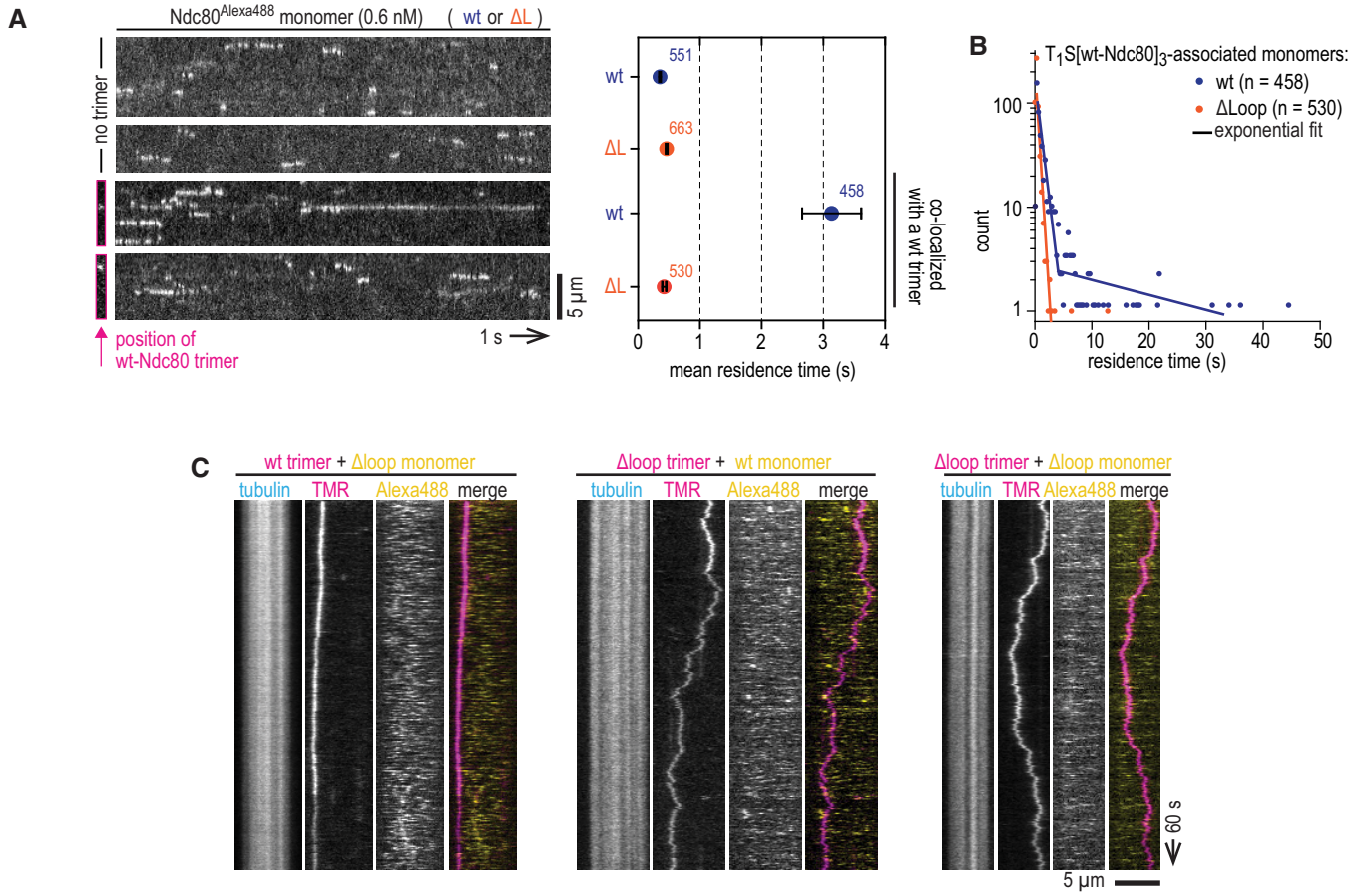

Figure EV4. Loop-dependent binding between Ndc80 monomers and trimers on microtubules.

A Supplementary information for Fig 5A–D. High-speed recordings to quantify residence time of wild-type and loopless Ndc80 monomers. The top two kymographs show a microtubule with monomers binding and unbinding. The lower two kymographs show the binding and unbinding of Ndc80 monomers to a microtubule with a Ndc80 trimer. Since trimers are practically motionless on this timescale, only their initial location was recorded and indicated. Corresponding mean residence times and SEM. are shown. The number of analyzed events is indicated. Scale bar: 5 µm.

B Distribution of residence times of wild-type and loopless Ndc80 monomers associating with microtubule-bound Ndc80 trimers. A single-exponential fit described the residence time of $Ndc80^{\Delta loop}$, likely corresponding to $Ndc80^{\Delta loop}$:microtubule off-rates. Residence time of full-length Ndc80 could be fitted with two exponents, likely corresponding to Ndc80:microtubule and Ndc80:trimer:microtubule off-rates.

C Typical kymographs showing Ndc80 trimers (magenta) and transiently binding Ndc80 monomers (yellow). Scale bars: vertical (100 s), horizontal (5 µm).

Source data are available online for this figure.

Figure EV5. Characterization of AB-849 and AB-850 in vitro.

A AB-849 and AB-850 recognize NDC80 in a HeLa cell lysate (lys) using immunoblotting. Recombinant Ndc80 complex (p) was used as a reference (see Fig 6A) Antibody dilutions are indicated and short (top panel) and long (bottom panel) exposures are shown.

B Experimental workflow to electroporate Ndc80 complexes with AB-849 or AB-850 into cells.

C The localization of AB-849, AB-850, NDC80, CENP-C, and DNA was analyzed using immunofluorescence microscopy. Representative cells are shown. Scale bar: 10 µm.

D Overview of mutants M15–M20, mutated in the epitope region of AB-849 to further test putative effects of the AB on the SAC.

E Time spent in mitosis in the presence or absence of nocodazole. Cells were electroporated with various Ndc80 constructs, when indicated following mixture with AB-849 or AB-850. Every dot represents a cell and red lines indicate median values. Effects of AB-849 on the time spent in mitosis were not recapitulated by any of the mutants M15–M20.

Source data are available online for this figure.

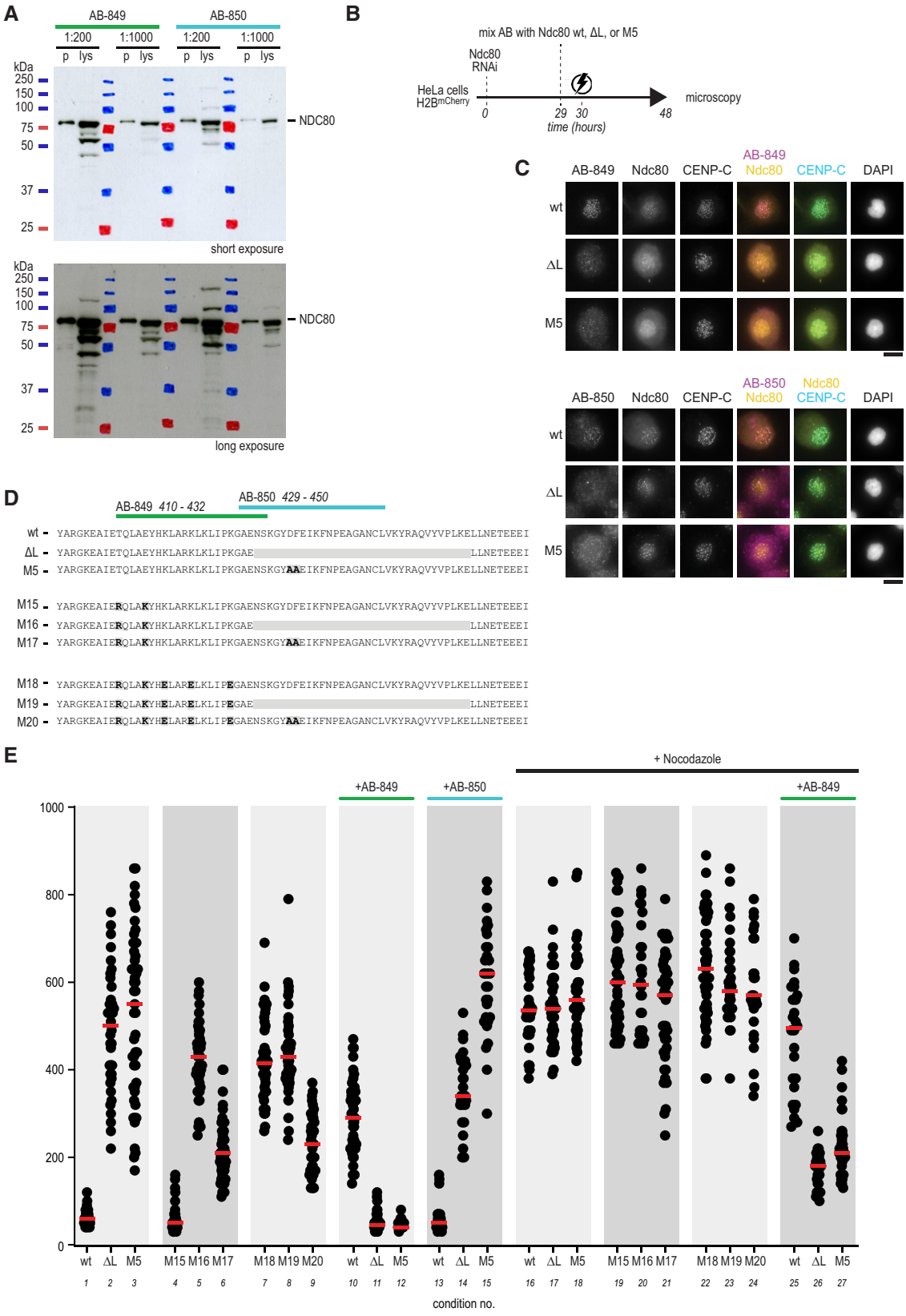

Figure EV5.

Author Query Form

Journal: EMBJ

Article: 2022112504

Dear Author,

During the copyediting of your manuscript the following queries arose.

Please refer to the query reference callout numbers in the page proofs and respond to each by marking the necessary comments using the PDF annotation tools.

Please remember illegible or unclear comments and corrections may delay publication.

Many thanks for your assistance.

AUTHOR: Please note that missing content in references have been updated where we have been able to match the missing elements without ambiguity against a standard citation database, to meet the reference style requirements of the journal. It is your responsibility to check and ensure that all listed references are complete and accurate.

Query reference	Query	Remarks